Theoretical and experimental study of surface and bulk contributions in resonant inverse photoemission of $CeRh_3$

T. Uozumi
College of Engineering, Osaka Prefecture University, Sakai, Osaka 599-8531, Japan

K. Kanai
RIKEN, Sayo-gun, Hyogo 679-5148, Japan

S. Shin and A. Kotani
Institute for Solid State Physics,University of Tokyo, Kashiwanoha, Kashiwa, Chiba 277-8581, Japan

G. Schmerber, J. P. Kappler, and J. C. Parlebas
IPCMS-GEMM, UMR 7504 CNRS, University Louis Pasteur, 23 rue du Loess, 67037 Strasbourg, France
(Received 21 June 2001; published 3 January 2002)

The surface and bulk sensitivity of resonant inverse photoemission (RIPE) spectroscopy is theoretically and experimentally studied for a typical mixed-valent compound $CeRh_3$ around the prethreshold region of the Ce $N_{4,5}$ edge. The strong resonance effects—the change of the intensity ratio between the f^1 and f^2 structures and the change of the spectral shape in the f^2 structure—are clearly found with the change of the excitation energy. The observed resonance behavior is successfully analyzed with an impurity Anderson model by explicitly considering both bulk and surface contributions in RIPE spectra. The explicit consideration of the surface contribution, in addition to the full-multiplet coupling effects in a Ce ion, is indispensable to reproduce the observed RIPE spectra for the whole excitation energy range around the prethreshold. The RIPE spectra of $CeRh_3$ around the giant resonance of the Ce $N_{4,5}$ edge are also calculated with explicit consideration of the surface contribution. The present calculation improves our previous one for the Ce $N_{4,5}$ RIPE spectra of $CeRh_3$ without the surface contribution. Moreover, the RIPE spectra of $CeRh_3$ at the Ce M_5 edge are also investigated by considering surface and bulk effects. We emphasize the importance of the surface contribution in the interpretation of the Ce M_5 RIPE spectra.

DOI: 10.1103/PhysRevB.65.045105 PACS number(s): 71.28.+d, 73.20.At, 78.70.En, 79.60.−i

I. INTRODUCTION

Cerium and its intermetallic compounds have attracted much interest because of their anomalous magnetic, electric, and thermal properties.[1] In these compounds, strongly correlated Ce $4f$ electrons play a crucial role in such anomalous properties through the hybridization of $4f$ electrons with conduction electrons. The compounds are then characterized according to the magnitude of the hybridization strength and their classification is made from a system with a mixed-valent character to that with almost localized $4f$ electrons. The former is often referred to as an α-like system, while the latter as a γ-like one, in analogy with α-Ce and γ-Ce, respectively.

High-energy spectroscopies, such as x-ray photoemission spectroscopy[2] (XPS) and x-ray absorption spectroscopy[3] (XAS), have played an important role in the investigation of electronic properties of Ce compounds.[4–6] In such studies, the information on the electronic structure of the compounds is derived from theoretical analyses of the spectra, where an impurity Anderson model is often employed in the calculations since it includes essential effects describing the electronic states of Ce compounds, the correlation between $4f$ electrons and the hybridization between $4f$ and conduction electrons.[7]

In recent years, it has been recognized that the surface of the α-like compounds has quite different electronic properties as compared to those of the bulk: the electronic structure of the surface resembles that of γ-like compounds because of the reduction of the hybridization strength and the lowering of $4f$ energy levels at the surface, both of which result in the stabilization of a localized $4f$ electron state.[8] This fact means that, without considering the surface and bulk sensitivity, we cannot directly derive the electronic structure of the bulk of α-like compounds from XPS studies, especially in the soft x-ray region.[9–11] Actually, considerable changes in the spectral shape of $3d$ XPS have been found for several α-like compounds when the surface and bulk sensitivity in the XPS measurements is controlled by changing the incident photon energy or by changing the escape angle of photoelectrons from a specimen.[8,12] This is in contrast with less-surface-sensitive measurements, such as XAS and x-ray emission spectroscopy (XES).

Resonant inverse photoemission (RIPE) spectroscopy is a new probe to investigate unoccupied electronic states of such systems.[13] The RIPE process is composed of two kinds of transition channels interfering with each other: one is the direct transition to the final state, $4f^n + e^- \rightarrow 4f^{n+1} + \omega$, and the other is the resonant transition $4f^n + e^- \rightarrow \underline{c}4f^{n+2} \rightarrow 4f^{n+1} + \omega$, where n means the configuration number of the $4f$ electrons in the initial state and $\underline{c}$ means a core hole resonantly excited in the intermediate state through the Cou-

lomb scattering by an incident electron. The first corresponds to the conventional inverse photoemission process, while the second occurs when the incident electron energy is tuned around the $c \rightarrow 4f$ absorption edge. Recently, RIPE measurements for several Ce compounds have been performed by Grioni *et al.* at the Ce M_5 edge[14] and by Kanai *et al.* at the Ce $N_{4,5}$ edge.[15–18] In these studies, the great ability of the RIPE technique has been testified, where considerable resonant enhancements of the photon signal intensities were observed around $c \rightarrow 4f$ absorption edges. Because of the element and orbital selectivity by the specific core excitation, only the photon signals related to $4f$ states can be enhanced in RIPE processes. Thus RIPE techniques are suitable for the investigation of the $4f$ electronic states of Ce compounds.

In order to quantitatively interpret RIPE spectra, especially for α-like compounds, both bulk and surface contributions should be taken into account in the analyses, because the RIPE spectroscopy is essentially a surface-sensitive technique. This fact cannot be overlooked especially in the interpretation of RIPE spectra at the Ce $N_{4,5}$ edge. The incident electron energy in this process is about 120 eV, so the incident electrons have a very short mean free path (about 5 Å). Thus a considerable surface contribution is expected in RIPE spectra at the Ce $N_{4,5}$ edge. In fact, Kanai *et al.*[15] have found considerable changes in the shape of the Ce $N_{4,5}$ RIPE spectra for $CePd_7$, a strongly hybridized system, and for α-Ce by changing the incidence angle of electrons.

The first theoretical analyses of RIPE spectra at the Ce M_5 edge for several Ce compounds were performed by Tanaka and Jo.[19] They found the possibility of a strong reduction of the hybridization strength in the intermediate state of the RIPE process from that in the initial state. According to their analyses, a scaling factor of 30% for the hybridization strength is required for $CeNi_2$ in order to theoretically reproduce the M_5 RIPE spectra and the factor of 50% for $CeRh_3$, for example. The change of the hybridization strength induced by the presence of a core hole and also by the change of the occupation number of $4f$ states was pointed out by Gunnarsson and Jepsen from first-principles calculations[20] and then has been considered by several authors in the analyses of various high-energy spectra.[11,19,21–25] However, the scaling factors of 30% for $CeNi_2$ and 50% for $CeRh_3$ proposed by Tanaka and Jo from their M_5 RIPE analyses seem to be too small, compared with the results of the analyses of other high-energy spectroscopic data.[11,24,25] The too small scaling factors by Tanaka and Jo may be caused by disregard of the surface contribution in their analyses. Thus we consider that the surface contribution should be taken into account even in the analyses of RIPE spectra at the Ce M_5 edge, at least for α-like compounds.

In a previous study, we have performed RIPE calculations for $CeRh_3$ at the giant resonance region of the Ce $N_{4,5}$ edge without considering the surface contribution, as a first step.[17] However, a full analysis including both surface and bulk contributions should be performed for the reason mentioned above. Very recently, we have analyzed the RIPE spectra in the prethreshold region of the Ce $N_{4,5}$ edge of $CePd_3$, and showed that it is essential to take into account both the surface and bulk contributions.[18] Thus, it should be checked that this is also the case for $CeRh_3$ from theoretical and experimental studies.

In this paper, theoretical and experimental studies on RIPE spectroscopy are reported for $CeRh_3$. For the purpose of clarifying the surface and bulk sensitivity in this process, we observe RIPE spectra at the prethreshold of the Ce $N_{4,5}$ edge of $CeRh_3$ and theoretically analyze the spectra by explicitly taking into account both surface and bulk contributions. The RIPE spectra around the prethreshold region of the Ce $N_{4,5}$ edge are especially suitable for this aim, since sharp resonance effects are expected in this region.[18] Moreover, the RIPE spectra at the Ce $N_{4,5}$ giant resonance and at the Ce M_5 edge of $CeRh_3$ are also calculated by including surface and bulk effects and are compared with the corresponding experimental data.[14,17] The rest of the paper is organized as follows: The experimental measurements and the results of RIPE spectra at the prethreshold region of the Ce $N_{4,5}$ edge of $CeRh_3$ are given in Sec. II. The theoretical model and the RIPE calculation are described in Sec. III. The calculated results of RIPE spectra for the prethreshold and giant regions of the Ce $N_{4,5}$ edge and for the Ce M_5 edge are shown and compared with corresponding experimental results in Sec. IV. Some discussions are given in Sec. V, and finally, we give a conclusion in Sec. VI.

II. EXPERIMENTS

Measurements of RIPE spectra are performed in an ultrahigh-vacuum chamber where the pressure is about 1×10^{-10} Torr under the operation of an electron gun. Samples are kept around 20 K by a closed-cycle ^{4}He refrigerator. A clean surface of the polycrystalline $CeRh_3$ sample is obtained by scraping the surface with a diamond file in an ultrahigh vacuum every $\sim$60 minutes at 20 K. The spectra of RIPE and inverse photoemission (IPE) are measured by the soft x-ray emission system which has a Rowland mounted-type spectrometer.[26] The E_F position is determined by referring to the Fermi edge in IPE spectra of Au which is evaporated on the sample holder.

Figure 1 shows the observed RIPE spectra of $CeRh_3$ at the prethreshold region of the Ce $N_{4,5}$ edge. The spectra for various incident electron energy E_{ex} from 105 eV to 115.4 eV are plotted as a function of the final-state energy with respect to the Fermi level, E_F. We find two remarkable structures in each spectrum. The peak just above the Fermi level corresponds to the f^1 final state, and the structure around 5 eV corresponds to the f^2 final state. Here we simply refer to these structures as the f^1 peak and f^2 structure, respectively. The intensity of the f^1 peak shows a sharp enhancement when the excitation energy E_{ex} is tuned around 107 eV and shows a relatively smaller enhancement around $E_{ex} = 112$ eV. The intensity of the f^2 structure, on the other hand, does not change strongly, though its energy and spectral shape change with the excitation energy. The excitation energy dependence of the intensities of the f^1 peak and the f^2 structure, i.e., constant final-state spectra (CFS), is shown in Fig. 2: The CFS for the f^1 and f^2 final states are obtained by measuring the RIPE intensity with the final-state energy between 0 and 2 eV and that between 3.75 and 5.75 eV,

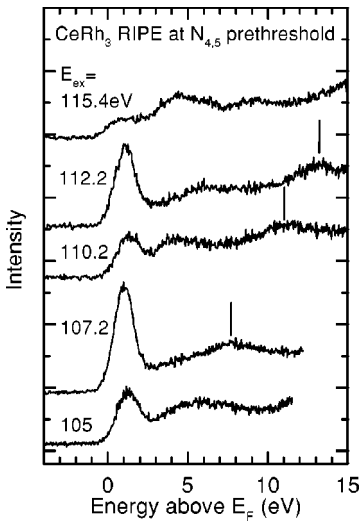

FIG. 1. The observed RIPE spectra of $CeRh_3$ around the prethreshold region of the Ce $N_{4,5}$ edge. The spectra for various excitation energy E_{ex} are plotted as a function of the final-state energy with respect to the Fermi energy E_F. The vertical bars are explained and discussed in Sec. V.

respectively. We see the characteristic behavior of the f^1 and f^2 intensities with the change of the excitation energy.

III. THEORETICAL MODEL

In this study, the resonant inverse photoemission spectra are analyzed by means of an impurity Anderson model including full multiplet coupling effects in a Ce ion. Our system is composed of $4f$, $4d$ core, $3d$ core states of a single Ce ion and conduction band states. The Hamiltonian is given by

$$H=\epsilon_f\sum_{\gamma} f^{\dagger}_{\gamma}f_{\gamma}+\sum_{k,\gamma}\epsilon_c(k)a^{\dagger}_{k\gamma}a_{k\gamma}+\frac{V}{\sqrt{N}}\sum_{k,\gamma}(f^{\dagger}_{\gamma}a_{k\gamma}+a^{\dagger}_{k\gamma}f_{\gamma})$$

$$+U_{ff}\sum_{\gamma>\gamma'} n_{f_\gamma}n_{f_{\gamma'}}-U_{fc}\sum_{\gamma,\xi} n_{f_\gamma}c_{\xi}c^{\dagger}_{\xi}+H_{mult}, \qquad (3.1)$$

where $f^{\dagger}_{\gamma}$ and $a^{\dagger}_{k\gamma}$ are electron creation operators for $4f$ and conduction band states, respectively, and $c^{\dagger}_{\xi}$ is an electron creation operator for $3d$ or $4d$ core states. The indices γ and

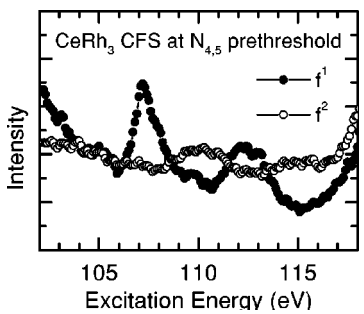

FIG. 2. The observed excitation energy dependence of the integrated intensities of the f^1 peak (solid circles) and f^2 structure (open circles) in the Ce $N_{4,5}$ prethreshold region of $CeRh_3$.

ξ of the operators represent both orbital and spin states, while the index k describes energy levels for discretized conduction band states below E_F $(k=1,\ldots,N)$. The effect of the conduction band states above E_F is disregarded, because their contribution is less important compared with that below E_F. The first and second terms are the one-particle energy of $4f$ and conduction band electrons, respectively, while the third term describes the hybridization interaction between $4f$ and conduction band states. In the second term, a constant density of states is assumed for the conduction band, and the discrete energy levels $\epsilon_c(k)$ are taken as

$$\epsilon_c(k)=E_F-\frac{W}{N}\left(k-\frac{1}{2}\right)\quad(k=1,\ldots,N), \qquad (3.2)$$

where W is the energy width from the bottom of the conduction band to the Fermi level E_F. In the present calculation, we choose W as 3.0 eV and discretize the conduction band into six levels $(N=6)$. The fourth term in Eq. (3.1) describes the repulsive Coulomb interaction between $4f$ electrons, and the fifth term describes the attractive core-hole potential for $4f$ electrons. The last term H_{mult} in Eq. (3.1) includes both multipole parts of the Coulomb interaction and the spin-orbit interaction. The Slater integrals F^k and G^k and the spin-orbit coupling constants ζ in H_{mult} are estimated through the Hartree-Fock-Slater (HFS) calculation for a Ce ion. The HFS values for various electronic configurations are listed in Table I, but the reduced values of Slater integrals from those in the table were used in the spectral calculations. The reason for this is an empirical inclusion of configuration interaction effects from the higher-basis configurations which are not included in our basis set described below. The scaling factor for the Slater integrals is taken as follows: $F^k(4f,4f)$ in the ground state and in the final state of RIPE spectra is scaled by 80%; $F^k(4f,4f)$, $F^k(4d,4f)$, and $G^k(4d,4f)$ in the intermediate state of the Ce $N_{4,5}$ RIPE spectra are scaled by 80%, 75%, and 66%, respectively; all of the Slater integrals in the intermediate state of the Ce M_5 RIPE spectra are scaled by 80%.

The wave function of the system is described as a linear combination of several electronic configurations. We describe the ground state $|g\rangle$ by a linear combination of f^0, $f^1\underline{v}$, and $f^2\underline{v}^2$ and the final states $|f\rangle$ of RIPE process by linear combinations of f^1, $f^2\underline{v}$, and $f^3\underline{v}^2$, where $\underline{v}$ means a hole in the conduction band below E_F. Similarly, the intermediate states with a core hole $\underline{c}$ are described by linear combinations of $\underline{c}f^2$ and $\underline{c}f^3\underline{v}$.

The model Hamiltonian in Eq. (3.1) includes several adjustable parameters: the $4f$ energy level ϵ_f with respect to the Fermi level, the hybridization strength V between $4f$ and conduction band states, the correlation energy U_{ff} between $4f$ electrons, and the core-hole potential energy U_{fc}. The values of such parameters are estimated mainly from combined analyses of $3d$ XPS and IPE spectra and are summarized in Table II for the bulk and surface states of $CeRh_3$.

Here we should mention about the configuration-dependent hybridization strength and the configuration-dependent Coulomb interaction assumed in the present calculation. The first, as mentioned in Sec. I, is induced by an

TABLE I. Slater intergrals (eV) and spin-orbit coupling constants (eV) for various electronic configurations of Ce ion. The values are estimated through the Hartree-Fock-Slater calculations. Note that the values scaled from those listed in this table are used in the spectral calculations. The Auger and radiative transitions concerning $N_{4,5}$ and M_5 RIPE processes are also listed here.

Configuration	$4f$-$4f$			$4f$-core					Spin-orbit	
	F^2	F^4	F^6						$\zeta(4f)$	
$4f^1$	–	–	–						0.087	
$4f^2$	10.223	6.347	4.548						0.074	
$4f^3$	7.692	4.693	3.341						0.058	
				F^2	F^4	G^1	G^3	G^5		$\zeta(4d)$
$4d^9 4f^2$	11.978	7.522	5.413	13.616	8.686	16.164	10.088	7.118	0.091	1.242
$4d^9 4f^3$	10.695	6.659	4.776	12.592	7.963	14.882	9.226	6.493	0.080	1.225
										$\zeta(3d)$
$3d^9 4f^2$	12.628	7.940	5.717	7.486	3.384	5.073	2.968	2.048	0.119	7.442
$3d^9 4f^3$	11.383	7.100	5.096	6.719	2.998	4.470	2.613	1.803	0.095	7.450

RIPE process	Auger R^k(core ϵg,$4f4f$) (eV)			Radiative (eV)	($\sqrt{\text{eV}}$)
	R^1	R^3	R^5	$R(c,4f)$	$R(\epsilon_g,4f)$
$4d^{10}4f^0\epsilon_g$-$4d^9 4f^2$-$4d^9 4f^1$	−0.8651	−0.4709	−0.3111	−0.7577	0.0761
$4d^{10}4f^1\epsilon_g$-$4d^9 4f^3$-$4d^{10}4f^2$	−0.8184	−0.4472	−0.2957	−0.7554	0.0722
$4d^{10}4f^2\epsilon_g$-$4d^{10}4f^3$	–	–	–	–	0.0649
$3d^{10}4f^0\epsilon_g$-$3d^9 4f^2$-$3d^{10}4f^1$	0.1735	0.1123	0.0804	0.1421	0.0021
$3d^{10}4f^1\epsilon_g$-$3d^9 4f^3$-$3d^{10}4f^2$	0.1539	0.0996	0.0712	0.1341	0.0020
$3d^{10}4f^2\epsilon_g$-$3d^{10}4f^3$	–	–	–	–	0.0020

appearance of a core hole and also by the change in the occupation number of $4f$ states. The appearance of the attractive core-hole potential leads a shrinkage of $4f$ states, which results in the reduction of the hybridization strength between $4f$ and conduction band states. On the other hand, when the number of $4f$ electrons is increased by the charge transfer from the conduction band to $4f$ states and also by the core-electron excitation to $4f$ states, the $4f$ wave function is somewhat delocalized due to the repulsion between $4f$ electrons, which results in an increase of the hybridization strength. Such effects can be included in the calculation by introducing scaling factors R_c and R_v (Ref. 22): the hybridization strength V in Table I, which is defined as that between $4f^0$ and $4f^1\underline{v}$ configurations, is scaled by R_c when a core hole is created and is scaled by $1/R_v^m$ when m electrons are added to $4f$ states. Thus the hybridization strength between $c\overline{4f^2}$ and $c\overline{4f^3}\underline{v}$ configurations in the intermediate state of the RIPE process, for example, is given by $(R_c/R_v^2)V$. In the present calculation, we choose (R_c,R_v) as $(0.7,0.8)$. The second, the configuration dependence of the Coulomb interaction, is also caused by the difference in the spatial extension of $4f$ states between the configurations with and without a core hole. We assume here that U_{ff} in the intermediate states with a core hole is larger than that in the initial and final states without a core hole. The consideration of such effects is important for consistent analyses of $3d$ XPS and IPE spectra of Ce compounds.[11,24]

TABLE II. Parameter values for bulk and surface states of $CeRh_3$. The values are estimated mainly from the combined analyses of $3d$ XPS and IPE spectra. In this study, only the values of $4f$ energy level ϵ_f and the hybridization strength V differ between bulk and surface states. The configuration dependence of V, through the scaling factor $(R_c,R_v)=(0.7,0.8)$, and that of U_{ff} are taken into account in the calculation.

	ϵ_f-E_F	V	U_{ff} (with a core hole)	$U_{fc}(4d)$	$U_{fc}(3d)$	W
Bulk	−1.2	0.54	5.5 (7.4)	9.5	10.8	3.0
Surface	−1.7	0.36	5.5 (7.4)	9.5	10.8	3.0

In this study, we also consider the bulk and surface contributions in RIPE spectra explicitly. Here the bulk and surface electronic states are assumed to be independently described by the Hamiltonian in Eq. (3.1) using different sets of parameter values. In the present calculation, however, we assume that only the values of the $4f$ energy level ϵ_f and the hybridization strength V differ between bulk and surface: $4f$ energy level ϵ_f(B) in bulk and ϵ_f(S) in the surface are chosen so that $\epsilon_f(\mathrm{B})>\epsilon_f(\mathrm{S})$ because of the surface $4f$-level shift, and the hybridization strength V(B) in bulk and V(S) in the surface are chosen so that $V(\mathrm{B})>V(\mathrm{S})$ because of the presence of vacuum at the surface. Such a theoretical treatment of bulk and surface electronic states has been successfully applied to combined analyses of $3d$ XPS and IPE spectrum of $CeRh_3$ (Ref. 11) and those of L_3 XAS, $3d$ XPS and bremstrahlung isochromat spectra (BIS) of $CePd_7$.[27]

The RIPE spectra are calculated as a function of the inci-

dent electron energy E_{ex} and emitted photon energy ω by the formula

$$F(\omega,E_{ex})=\sum_f \left|\langle f|T_R+T_R\frac{1}{E_{ex}+E_g-H+i\Gamma}V_A^\dagger|g\rangle\right|^2 \times\delta(E_{ex}+E_g-\omega-E_f), \quad (3.3)$$

where E_g and E_f are, respectively, the ground-state and final-state energies, T_R describes the electric dipole transitions, and $V_A^\dagger$ describes the resonant excitation of the system through the Coulomb scattering between core and incident electrons. The first term in Eq. (3.3) represents the direct transition $\epsilon_l+4f^n\rightarrow 4f^{n+1}+\omega$, while the second term represents the resonant transition $\epsilon_l+4f^n\rightarrow \underline{c}4f^{n+2}\rightarrow 4f^{n+1}+\omega$, where ϵ_l means incident electrons with the angular momentum l. In the RIPE processes considered here, incident electrons ϵ_s, ϵ_d, ϵ_g, and ϵ_i can contribute to the resonant excitation. However, in this study, we only consider the excitation by incident electrons ϵ_g which has the largest contribution to the spectra in the present case. In Eq. (3.3), Γ is a constant lifetime of the intermediate state and is chosen to be 2.0 eV and 0.15 eV for $N_{4,5}$ resonant excitation in the giant and the prethreshold regions, respectively, and to be 0.5 eV for M_5 resonant excitation.

IV. RESULTS

A. Ground state in bulk and surface

In this study, the values of adjustable parameters included in the Hamiltonian in Eq. (3.1) are chosen as those in Table II, which are estimated as follows: The parameter values for bulk of $CeRh_3$ are estimated through the combined analyses of *high-energy* $3d$ XPS (Ref. 28) observed around the Ce L_3 edge and BIS (Ref. 29) observed with incident electron energy about 1500 eV. In the former analysis, the detail of the resonance effects on the spectral shape has been neglected for simplicity. Then the parameter values for surface of $CeRh_3$ are estimated so that *low-energy* $3d$ XPS observed with incident photon energy 1400 eV (Ref. 29) and the *low-energy* IPE spectrum observed with incident electron energy 80 eV (Ref. 17) are simultaneously reproduced by superpositions of calculated surface and bulk contributions, where the weights of surface and bulk contributions are assumed as 30 and 70 for $3d$ XPS and 50 and 50 for IPE spectra [see the bottom of Figs. 5(a) and 5(b) for the *low-energy* IPE analysis].

The ground state is independently calculated for surface and bulk by numerically diagonalizing the Hamiltonian in Eq. (3.1). The obtained character of the ground state is summarized in Table III, which clearly shows the mixed-valent character of bulk electronic states of $CeRh_3$ and also shows the γ-like character of surface electronic states. The γ-like character in the surface is due to the surface $4f$-level shift [$\epsilon_f(\mathrm{S})<\epsilon_f(\mathrm{B})$] and the reduction of the hybridization strength [$V(\mathrm{S})<V(\mathrm{B})$] in the surface (see also Table II).

TABLE III. Characters of ground state in bulk and surface states of $CeRh_3$. The weights for the basis configurations and the averaged $4f$ electron number in the ground state are shown.

	Weights			n_f
	f^0	$f^1\underline{v}$	$f^2\underline{v}^2$	
Bulk	0.25	0.64	0.11	0.86
Surface	0.13	0.78	0.09	0.96

B. $N_{4,5}$ RIPE spectra at the prethreshold region

Figure 3 shows theoretical RIPE spectra (solid lines) at the prethreshold region of the Ce $N_{4,5}$ edge, where the spectra for incident electron energy E_{ex} from 105.2 eV to 113.2 eV are plotted as a function of the final-state energy E_f with respect to the theoretical Fermi level E_F. The origin of the excitation energy E_{ex} in the calculation is adjusted to fit the experimental conditions. In this calculation, the surface (dotted lines) and bulk (dashed lines) contributions are independently calculated by Eq. (3.3) and are convoluted with a Gaussian function which has the energy-dependent half-width $0.5+0.01|E-E_F|^2$ eV at half-maximum. Then each total RIPE spectrum is obtained as a superposition of the corresponding surface and bulk contributions, where the weight of 50 and 50 is assumed as the surface and bulk

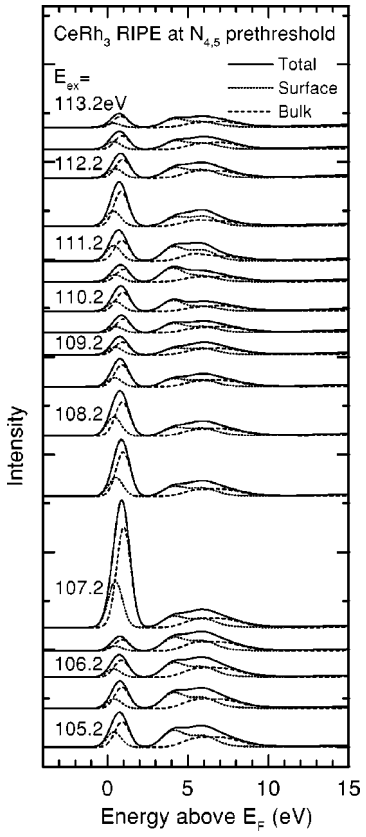

FIG. 3. The calculated RIPE spectra of $CeRh_3$ around the prethreshold region of the Ce $N_{4,5}$ edge. The total spectra (solid lines) for various excitation energy E_{ex} are obtained as a superposition of the surface (dotted lines) and bulk (dashed lines) contributions with the surface and bulk weight of 50 and 50, respectively.

sensitivity, respectively. This weight is determined so as to give a good agreement between the calculated and experimental RIPE spectra, as well as from a rough estimation based on the mean free path of the incident electron (see Ref. 16).

In this figure, both surface and bulk contributions show the f^1 peak and the f^2 structure. We find that the energy position of the f^2 structure of surface spectra is in the low-energy side of that of bulk spectra. This is mainly due to the lowering of the $4f$ level ϵ_f at the surface, where the energy position of the f^2 structure is roughly given by $\epsilon_f + U_{ff}$ above E_F. We also note that the f^2 structures in both surface and bulk contributions have a double-peak structure, although such structure is not clearly resolved in the experiment (Fig. 1). The double-peak structure originates from the energy splitting of $4f^2$ multiplet terms: the lower-energy peak corresponds to multiplet terms ^3H, ^3F, and ^1G, while the higher-energy peak corresponds to multiplet terms ^1D, ^1I, and ^3P. It is shown that the experimental resonance behavior in Fig. 1 is almost reproduced by the total RIPE spectra for the whole excitation energy: the sharp enhancement around $E_{ex}=107$ eV and the relatively weaker enhancement around $E_{ex}=112$ eV for the f^1 peak; the change in the spectral shape of the f^2 structure above $E_{ex}=110.2$ eV, though the peak energy position of the f^2 structure for $E_{ex}=107.2$ eV is somewhat different from the experimental result. It is to be emphasized that if the surface contribution is disregarded, the energy position of the f^2 structure is too high (except for the case of 107.2 eV). This fact clearly shows that the considerable surface contribution is included in RIPE spectra around the Ce $N_{4,5}$ prethreshold region. The reason for the disagreement of the calculated and experimental f^2 spectra for $E_{ex}=107.2$ eV will be discussed in Sec. V.

Figure 4 shows the calculated excitation energy dependence of the f^1 peak and f^2 structure, where the f^1 (solid circles) and f^2 (open circles) curves for total, surface, and bulk spectra are respectively plotted in Figs. 4(a), 4(b), and 4(c). We note that the f^1 and f^2 curves for total spectra in Fig. 4(a) reproduce fairly well the observed CFS in Fig. 2: the sharp resonance around $E_{ex}=107$ eV, relatively weaker resonance around $E_{ex}=112$ eV of f^1 peak, and the intensity ratio between the f^1 and f^2 curves.

The resonance behavior obtained above is explained in the same way as the case of $CePd_3$.[18] The sharp resonance of the f^1 peak around $E_{ex}=107$ eV occurs through the transition $4f^0+e^- \rightarrow \underline{4d}4f^2(^4G) \rightarrow 4f^1(^2F)+\omega$. Although the direct transition from $\underline{4d}4f^2(^4G)$ to $4f^1(^2F)+\omega$ is dipole forbidden, this transition can occur passing through the $\underline{4d}4f^2(^2G)$ component which is slightly mixed with $\underline{4d}4f^2(^4G)$ owing to the spin-orbit interaction. The change in the spectral shape of the f^2 structure with the change of the excitation energy is caused by the multiplet selection rule in the transition $4f^1+e^- \rightarrow \underline{4d}4f^3 \rightarrow 4f^2+\omega$ and also by the change of the *effective* surface and bulk sensitivity around the Ce $N_{4,5}$ prethoreshold region.

In the case of $CePd_3$, the *effective* surface and bulk sensitivity is strikingly changed at some specific excitation energies in the Ce $N_{4,5}$ prethreshold region, as discussed in Ref. 18. This is due to the fact that the resonance behavior in the Ce $N_{4,5}$ prethreshold region strongly reflects the ground-state character. Thus the contributions from the surface with γ-like character or from the bulk with α-like character can be selectively enhanced by choosing a specific excitation energy corresponding to a characteristic multiplet of the intermediate state, such as the $\underline{4d}4f^2(^4G)$. However, as shown in Figs. 4(b) and 4(c), the resonance behavior of the surface and bulk contributions of $CeRh_3$ does not have a strong contrast compared with the case of $CePd_3$. This is due to the fact that the surface state obtained in the present calculation still has a considerable $4f^0$ weight of 13% as shown in Table III. Thus, the selectivity of the surface and bulk contributions by choosing a specific intermediate state seems to be weakened for $CeRh_3$.

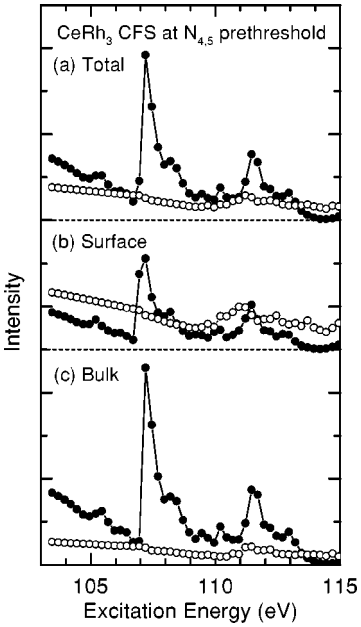

FIG. 4. The calculated excitation energy dependence of the integrated intensities of the f^1 peak and f^2 structure in the Ce $N_{4,5}$ prethreshold region of $CeRh_3$. The f^1 (solid circles) and f^2 (open circles) curves in the total contribution (a) are calculated as a superposition of the corresponding curves in the surface (b) and bulk (c) contributions with the surface and bulk weight of 50 and 50, respectively.

C. $N_{4,5}$ RIPE spectra at giant resonance

Figure 5(a) shows theoretical RIPE spectra of $CeRh_3$ at the Ce $N_{4,5}$ giant resonance, where the incident electron energy is changed from 114 eV to 126 eV. The spectra are plotted as a function of the final-state energy E_f with respect to the theoretical Fermi level E_F. In this calculation, total RIPE spectra (solid lines) are obtained as a superposition of the surface (dotted lines) and bulk (dashed lines) contributions with the weight of 50/50 which is the same as that used in the RIPE calculation at the $N_{4,5}$ prethreshold region. As in Sec. IV B, the surface and bulk contributions are independently calculated by Eq. (3.3) and are convoluted with a

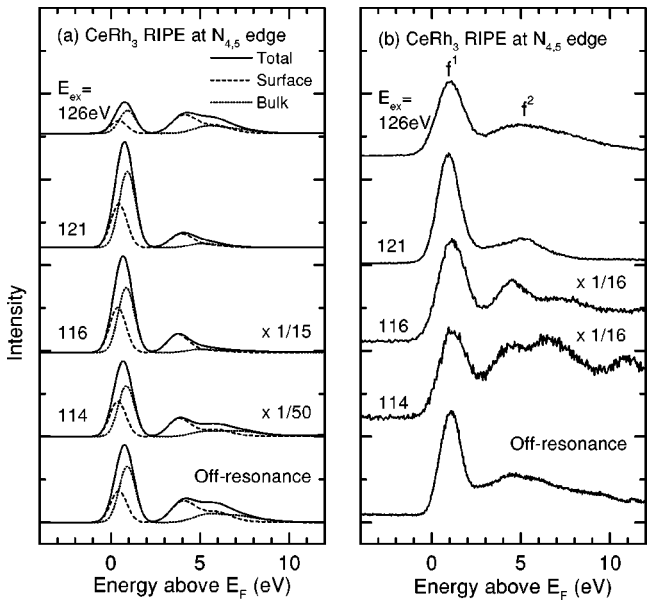

FIG. 5. The calculated (a) and experimental (b) (Ref. 17) RIPE spectra of $CeRh_3$ around the Ce $N_{4,5}$ giant resonance region. The total spectra (solid lines) for various excitation energy E_{ex} in (a) are obtained as a superposition of the surface (dotted lines) and the bulk (dashed lines) contributions with the surface and bulk weight of 50 and 50, respectively. The off-resonance IPE spectra are also shown in the bottom of (a) and (b).

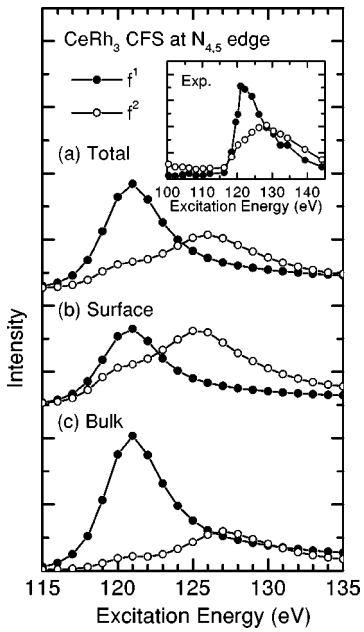

FIG. 6. The calculated excitation energy dependence of the integrated intensities of the f^1 peak and f^2 structure in the Ce $N_{4,5}$ giant resonance region of $CeRh_3$. The f^1 (solid circles) and f^2 (open circles) curves in the total contribution (a) are calculated as a superposition of the corresponding curves in the surface (b) and bulk (c) contributions with the surface and bulk weight of 50 and 50, respectively. The inset shows the experimental curves (Ref. 17).

Gaussian function which has the energy-dependent half-width $0.5+0.01|E-E_F|^2$ eV at half-maximum. It is found that the total RIPE spectra in Fig. 5(a) are in good agreement with our previous data in Fig. 5(b) from Ref. 17.

In our previous study,[17] we have calculated RIPE spectra at the Ce $N_{4,5}$ giant resonance of $CeRh_3$ with a *single* parameter set as a first step of the analysis. Although the observed resonance behavior of RIPE spectra was almost reproduced in that calculation, there remained some problems: (i) The energy position of the f^2 structure is higher by about 1.5 eV than that observed experimentally. (ii) The average number of $4f$ electrons, $n_f=1.0$, in the ground state does not agree with the strongly mixed-valent character of $CeRh_3$. Such problems in the previous study arise mainly from the use of the *single* parameter set which was estimated from the analysis of *low-energy* $3d$ XPS.[29]

When we analyze *low-energy* $3d$ XPS without considering the surface contribution, the derived parameter set has an intermediate character between bulk and surface because of a considerable surface contribution included in *low-energy* $3d$ XPS. Therefore, if we calculate *surface sensitive* $N_{4,5}$ RIPE spectra using this parameter set, it will bring some discrepancies between theory and experiment. Such situations in the RIPE analysis of Ce compounds would be remarkable for α-like compounds, since the electronic state in the surface quite differs from that in the bulk of such compounds. However, the problems (i) and (ii) in the previous study are largely improved in the present study: (i) The f^2 structure in Fig. 5(a) is largely contributed from the surface. Then, as a result of the superposition, the energy position of the f^2 structure in the total spectra is lowered from the previous calculation. This is due to the fact that the energy position of the f^2 structure is roughly given by ϵ_f+U_{ff} and that $\epsilon_f(\mathrm{S}) < \epsilon_f(\mathrm{B})$. (ii) The average number of $4f$ electrons 0.86 is obtained for the ground state in bulk, which agrees with the strongly mixed-valent character of $CeRh_3$.

Figure 6(a) shows the calculated excitation energy dependence of the integrated intensities of the f^1 peak (solid circles) and the f^2 structure (open circles) in RIPE spectra at the Ce $N_{4,5}$ giant resonance region of $CeRh_3$. The energy separation and the intensity ratio between the peaks in the f^1 and f^2 curves are in good agreement with our previous data shown in the inset of Fig. 6 from Ref. 17. We should remember that the total curves in Fig. 6(a) are obtained as the superposition of the surface (b) and bulk (c) contributions with a weight of 50/50. The resonance enhancement in the f^1 curve around $E_{ex}=121$ eV is largely contributed from the bulk (c), since this enhancement is due to the resonance $f^0+e^-\rightarrow \underline{4d}f^2\rightarrow f^1+\omega$. On the other hand, the resonance enhancement in the f^2 curve around $E_{ex}=126$ eV is largely contributed from the surface (b), since this enhancement is due to the resonance $f^1\underline{v}+e^-\rightarrow \underline{4d}f^3\underline{v}\rightarrow f^2\underline{v}+\omega$. Then, as a result of the superposition of bulk and surface contributions, the total curves reproduce the observed data.[17]

D. M_5 RIPE spectra

Figure 7 shows calculated CFS around the Ce M_5 edge of $CeRh_3$, where (a), (b), and (c) show the total, surface, and bulk contributions, respectively. In the resonance around the Ce M_5 edge, the energy of the incident electrons is about 890

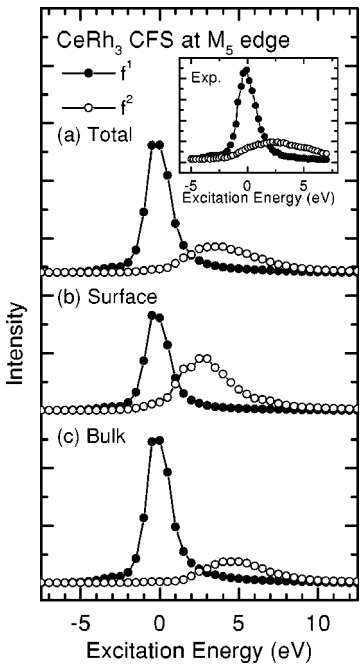

FIG. 7. The calculated excitation energy dependence of the integrated intensities of the f^1 peak and f^2 structure around the Ce M_5 edge of $CeRh_3$. The f^1 (solid circles) and f^2 (open circles) curves in the total contribution (a) are calculated as a superposition of the corresponding curves in the surface (b) and bulk (c) contributions with the surface and bulk weight of 30 and 70, respectively. The inset shows the experimental curves (Ref. 14).

eV and thus the electrons have a longer mean free path than that in the Ce $N_{4,5}$ resonance. However, we assume that RIPE spectra around the Ce M_5 edge still have an appreciable surface contribution. Then the total CFS in Fig. 7(a) are calculated as a superposition of surface (b) and bulk (c) contributions with a weight of 30/70. In this figure, the integrated intensities of the f^1 peak (solid circles) and the f^2 structure (open circles) are plotted as a function of the excitation energy. It is found that the f_1 and f_2 curves in Fig. 7(a) are in good agreement with CFS observed by Grioni *et al.*,[14] which is shown in the inset of Fig. 7: especially, (i) the ratio of maximum intensities between f^1 and f^2 curves, (ii) the broad band structure in the f^2 curve, and (iii) the energy difference between the peak positions of the f^1 and f^2 curves, which is about 3 eV as found from the inset. In this way, the observed M_5 RIPE spectra of $CeRh_3$ can be reproduced by assuming the existence of the surface contribution in the spectra. The validity of our interpretation proposed here will be further discussed in Sec. V.

V. DISCUSSION

In Sec. IV B we have seen that the observed resonance behavior in RIPE spectra at the prethreshold region of the Ce $N_{4,5}$ edge is almost reproduced with the present theoretical treatment explicitly considering both surface and bulk contributions. However, there was some discrepancies between theory and experiment with respect to the energy position of the f^2 structure in the RIPE spectrum for $E_{ex}=107.2$ eV (see Figs. 1 and 3). This may be caused by a normal emission process which is not taken into account in the present calculation. In fact, the structure marked by the vertical bar in the RIPE spectrum for $E_{ex}=107.2$ eV in Fig. 1 shifts toward the high-energy side almost linearly with the excitation energy, which means that the emitted photons related to such a structure have a constant energy against the change of excitation energy. The structure thus can be attributed to a kind of normal emission process in the RIPE process. Although we do not exactly know what kind of a decay channel causes such a process, a tunneling process of a $4f$ electron to a continuum state in the intermediate state may contribute to such a decay process. We consider that such a tunneling as $\underline{4d}4f^{n+2} \rightarrow \underline{4d}4f^{n+1}+\upsilon$ can occur even in the prethreshold excitation region, assisted by the Coulomb repulsion between $4f$ electrons overpopulated in the intermediate state of RIPE process, where υ means an electron in the continuum state. Then a photon emitted through the transition $\underline{4d}4f^{n+1}+\upsilon \rightarrow 4f^n+\upsilon+\omega$ has a constant energy. However, such a normal-like structure is not found in RIPE spectra of $CePd_3$. Thus the process mentioned above would depend on the electronic structure of the compounds.

In Sec. IV D, we have shown that also M_5 RIPE spectra of $CeRh_3$ can be reproduced by explicitly considering the surface and bulk contributions. However, as mentioned in Sec. I, another mechanism, a drastic reduction of the hybridization strength in the intermediate state, was proposed by Tanaka and Jo in order to interpret the M_5 RIPE spectra. From now on, we focus our discussion on the validity of our interpretation about the M_5 RIPE spectra.

First, it should be noted that the energy difference between the peaks of the f^1 and f^2 curves in the bulk CFS in Fig. 7(c) is about 4.5 eV, although the corresponding basis configurations $\underline{3d}f^2$ and $\underline{3d}f^3\underline{\upsilon}$ in the intermediate state have a far smaller configuration-averaged energy difference $|\epsilon_f+W/2+2U_{ff}(c)-U_{fc}(3d)|=0.5$ eV. This reflects the strong hybridization effect in the intermediate state. The hybridization strength $V_m(\mathrm{B})$ between $\underline{3d}f^2$ and $\underline{3d}f^3\underline{\upsilon}$ for bulk is now scaled by the factor $R_c/R_\upsilon^2 \sim 1.1$ from $V(\mathrm{B})$ and is given by $V_m(\mathrm{B})=0.59$ eV. It should be emphasized that $V_m(\mathrm{B})$ in our calculation is not decreased but increased by 10% from $V(\mathrm{B})$, which means R_c and R_υ effects almost cancel out with each other. The effective hybridization strength $\sqrt{N_f-2}V_m(\mathrm{B})$ between $\underline{3d}f^2$ and $\underline{3d}f^3\underline{\upsilon}$ configurations then becomes 2.0 eV, which mainly causes the large energy separation of $\sim$4.5 eV between the peaks of the f^1 and f^2 curves in Fig. 7(c). This fact illustrates a theoretical difficulty in the quantitative interpretation of M_5 RIPE spectra without assuming a drastic reduction of the hybridization strength in the intermediate state, if we attempt to reproduce observed M_5 RIPE spectra by considering only bulk contribution.

The assumption of the drastic reduction of the hybridization strength was proposed by Tanaka and Jo.[19] Such an effect certainly gives a smaller energy separation between the peaks of the f^1 and f^2 curves, which can be imagined from Fig. 7(b): the smaller hybridization $[V_m(\mathrm{S})=0.40$ eV$]$ gives the smaller energy separation of $\sim$2.8 eV. In this case, how-

ever, other parameters such as ϵ_f and U_{ff} should be further tuned to reproduce also the intensity ratio of the curves. On the other hand, what we propose in this paper is that the surface contribution still exists even in the M_5 RIPE spectra, and then the discrepancies between experiment (the inset in Fig. 7) and calculated CFS of bulk in Fig. 7(c) can be removed by superposing the surface curves in Fig. 7(b).

We have a few grounds to emphasize the validity of our analysis with the surface and bulk contributions, in addition to the consistency through the RIPE analyses given in the present study. First, the ratio $V_m(\mathrm{B})/V(\mathrm{B}) \sim 1.1$ in our model agrees with the ratio ~ 1.2 obtained by Gunnarson and Jepsen for α-Ce from the first-principles calculation.[20] Here we should pay attention to only the tendency of the change in the hybridization strength $[V_m(\mathrm{B})/V(\mathrm{B}) \geqslant 1]$ since their calculation was not done for $CeRh_3$. On the other hand, the ratio ~ 0.5 assumed by Tanaka and Jo[19] has the opposite tendency to this one. In our opinion, the ejection of a core hole surely leads to a reduction of the hybridization strength, on the one hand, but it is recovered by the additional two $4f$ electrons in the intermediate state on the other hand. As a result of the cancellation between both effects, $V_m(\mathrm{B})$ should not be much changed from $V(\mathrm{B})$. The second ground is a very recent calculation of the resonant x-ray photoemission spectra (RXPS) of $CeRh_3$ by Ogasawara *et al.*[25] They have shown that *bulk sensitive* RXPS around the Ce L_3 edge[28] can be reproduced by an impurity model which is essentially the same as our model except for the explicit consideration about the surface contribution. In their calculation, the factors (R_c, R_v) were chosen to be (0.7,0.8), and good agreement between theory and experiment was obtained. Thus, we consider that an appreciable surface contribution should be included even in the M_5 RIPE spectra. This fact should be explicitly considered in the RIPE analyses especially for α-like compounds.

We have given above a few grounds to support our treatment in the RIPE analyses. However, our model includes a superposing factor of the surface and bulk contribution as an adjustable parameter, which is not established in experimental studies. It is a crucial problem in the core-level spectroscopy to clarify the degree of configuration dependence of the hybridization strength since the accuracy of the information on electronic properties derived from the study greatly depends on the detailed comparison between experiments and theories. Therefore, it should be experimentally checked by performing measurements on the incidence angle dependence of M_5 RIPE spectra, especially for α-like compounds. Another check for our model is bulk-sensitive measurements such as resonant x-ray emission spectroscopy. We hope that such measurements will be carried out soon.

VI. SUMMARY AND CONCLUSION

In this study RIPE spectra around the Ce $N_{4,5}$ edge and the Ce M_5 edge are studied for a typical mixed-valent compound $CeRh_3$. In the experimental part, on the one hand, strong resonance effects are found in RIPE spectra around the prethreshold region of the Ce $N_{4,5}$ edge. In the theoretical part, on the other hand, RIPE processes are investigated with the impurity Anderson model by explicitly considering the surface and bulk contributions.

The observed resonance behavior of RIPE spectra around the prethrethold region is almost reproduced by the calculated spectra including both surface and bulk contributions with a weight of 50/50. The RIPE spectra around the $N_{4,5}$ giant resonance are also reproduced as the superposition of surface and bulk contributions with the same weight of 50/50. The present calculation greatly improves the previous results for $CeRh_3$ without considering the surface contribution. The present model also works in the interpretation of RIPE spectra around the Ce M_5 edge. In this analysis, we propose a new interpretation for M_5 RIPE spectra, where the shape of CFS are appreciably influenced by the surface contribution. From the analyses of the spectra, we have derived the bulk and surface electronic structure of $CeRh_3$. The average number of $4f$ electrons is estimated to be 0.86 for the bulk of $CeRh_3$, which is in agreement with the mixed-valent character of this compound. The γ-Ce-like character is also obtained for the surface of $CeRh_3$.

ACKNOWLEDGMENTS

The authors would like to thank Dr. H. Ogasawara for his valuable discussions. This work is partly supported by a Grant-in-Aid for Scientific Research from the Ministry of Education, Culture, Sports, Science and Technology in Japan.

[1] See, for instance, *Valence Fluctuations in Solids*, edited by L. M. Falicov, W. Henke, and M. B. Maple (North-Holland, Amsterdam, 1981).

[2] J. C. Fuggle, F. U. Hillebrecht, Z. Zolnierek, R. Lässer, Ch. Freiburg, O. Gunnarsson, and K. Schönhammer, Phys. Rev. B **27**, 7330 (1983).

[3] G. Kaindl, G. Kalkowski, W. D. Brewer, B. Perscheild, and F. Holtzberg, J. Appl. Phys. **55**, 1910 (1984).

[4] *Core-Level Spectroscopy in Condensed Systems*, edited by J. Kanamori and A. Kotani (Springer-Verlag, Berlin, 1988).

[5] A. Kotani, T. Jo, and J. C. Parlebas, Adv. Phys. **37**, 37 (1988).

[6] J. W. Allen, S. J. Oh, O. Gunnarsson, K. Schönhammer, M. B. Maple, M. S. Torikachvili, and I. Lindau, Adv. Phys. **35**, 275 (1986).

[7] O. Gunnarsson and K. Schönhammer, Phys. Rev. B **28**, 4315 (1983).

[8] C. Laubschat, E. Weschke, C. Holtz, M. Domke, O. Strebel, and G. Kaindl, Phys. Rev. Lett. **65**, 1639 (1990).

[9] A. Sekiyama, T. Iwasaki, K. Matsuda, Y. Saitoh, Y. Ônuki, and S. Suga, Nature (London) **403**, 396 (2000).

[10] S. Suga and A. Sekiyama, J. Electron Spectrosc. Relat. Phenom. **114-116**, 659 (2001).

[11] L. Duò, P. Vavassori, L. Braicovich, N. Witkowski, D. Malterre, M. Grioni, Y. Baer, and G. L. Olcese, Z. Phys. B **103**, 63 (1997).

[12] L. Braicovich, N. B. Brookes, C. Dallera, M. Salvietti, and G. L. Olcese, Phys. Rev. B **56**, 15 047 (1997).
[13] P. Weibel, M. Grioni, D. Malterre, B. Dardel, and Y. Baer, Phys. Rev. Lett. **72**, 1252 (1994).
[14] M. Grioni, P. Weibel, D. Malterre, and Y. Baer, Phys. Rev. B **55**, 2056 (1997), and references therein.
[15] K. Kanai, Y. Tezuka, M. Fujisawa, Y. Harada, S. Shin, G. Schmerber, J. P. Kappler, J. C. Parlebas, and A. Kotani, Phys. Rev. B **55**, 2623 (1997).
[16] K. Kanai, Y. Tezuka, H. Ishii, S. Nozawa, S. Shin, A. Kotani, G. Schmerber, J. P. Kappler, and J. C. Parlebas, J. Electron Spectrosc. Relat. Phenom. **92**, 81 (1998).
[17] K. Kanai, Y. Tezuka, T. Terashima, Y. Muro, M. Ishikawa, T. Uozumi, A. Kotani, G. Schmerber, J. P. Kappler, J. C. Parlebas, and S. Shin, Phys. Rev. B **60**, 5244 (1999).
[18] K. Kanai, T. Terashima, A. Kotani, T. Uozumi, G. Schmerber, J. P. Kappler, J. C. Parlebas, and S. Shin, Phys. Rev. B **63**, 033106 (2001).
[19] A. Tanaka and T. Jo, J. Phys. Soc. Jpn. **65**, 615 (1996).
[20] O. Gunnarsson and O. Jepsen, Phys. Rev. B **38**, 3568 (1998).
[21] T. Mizokawa and A. Fujimori, Phys. Rev. B **48**, 14 150 (1993).
[22] K. Okada and A. Kotani, J. Electron Spectrosc. Relat. Phenom. **71**, R1 (1995).
[23] M. Nakazawa, S. Tanaka, T. Uozumi, and A. Kotani, J. Phys. Soc. Jpn. **65**, 2303 (1996).
[24] N. Witkowski, F. Bertran, and D. Malterre, Phys. Rev. B **56**, 15 040 (1997).
[25] H. Ogasawara, A. Kotani, P. Le Fèvre, D. Chandesris, and H. Magnan, Phys. Rev. B **62**, 7970 (2000).
[26] S. Shin *et al.*, Rev. Sci. Instrum. **66**, 1584 (1995).
[27] Y. Iwamoto, M. Nakazawa, A. Kotani, and J. C. Parlebas, J. Phys.: Condens. Matter **7**, 1149 (1995).
[28] P. Le Fèvre, H. Magnan, and D. Chadesris, J. Vogel, V. Formoso, and F. Comin, Phys. Rev. B **58**, 1080 (1998).
[29] E. Weschke, C. Laubschat, R. Ecker, A. Höhr, M. Domke, G. Kaindl, L. Severin, and B. Johansson, Phys. Rev. Lett. **69**, 1792 (1992).